Towards Additive Manufacturing Based Packaging of Mm-Wave Antenna Arrays and Beamformer ICs

Ruoke Liu, Gokhan Mumcu, and Jing Wang
Department of Electrical Engineering, Center for Wireless and Microwave Information Systems,
University of South Florida
Tampa, FL, USA
rliu3@usf.edu

2024 IEEE Wireless and Microwave Technology Conference (WAMICON) | 979-8-3503-4494-3/24/$31.00 ©2024 IEEE | DOI: 10.1109/WAMICON60123.2024.10522864

***Abstract*—Laser enhanced direct print additive manufacturing (LE-DPAM) technology has recently been demonstrated to achieve success in packaging of antennas with phase shifters to realize passive phased antenna arrays (PAAs). Utilizing LE-DPAM for PAAs operating in mm-wave bands brings out new challenges that need to be addressed. These challenges are associated with smaller antenna and feature sizes needed for mm-wave band operation, necessity of active circuits for amplification, and number of pads, pad size and pad locations of mm-wave beamformer IC packages. This paper presents our initial progress in scaling LE-DPAM based packaging of PAAs into the mm-wave band operation through consideration and demonstration of discrete components (i.e. antenna array elements and beamformer ICs) that form the PAA structure. Specifically, a stand-alone, passive, 2×2 LE-DPAM based 26 GHz antenna subarray is investigated for its performance. In addition, a 24.5 GHz – 27 GHz beamformer IC is packaged in a stand-alone test article using LE-DPAM and investigated for its mm-wave performance and thermal aspects.**

Keywords—3D printing, IC packaging, mm-wave, phased antenna array, thermal management

I. Introduction

Structural integration of integrated circuits (ICs) and passive circuit components using additive manufacturing have garnered recent interest in the RF and microwave packaging community [1-4]. This interest is motivated by the fact that additive manufacturing offers several capabilities that are not available in traditional manufacturing such as non-standardized material thicknesses, variation of material properties in and out of plane, number of material layers, and 3D geometrical shapes [4]. Our recent research work has investigated the design and manufacturing of antennas and antenna arrays that fully take advantages of additive manufacturing. By investigating and employing laser-enhanced direct print additive manufacturing (LE-DPAM) technology, we demonstrated fully printed antenna elements operating in the Ku and X bands that are integrated with polarization selection switches and phase shifters, respectively [5, 6]. On the other hand, employing additive manufacturing within mm-wave band for structural integration of antenna arrays and integrated ICs faces unique challenges due to the smaller feature sizes, compactness of the antenna arrays, and necessity of utilizing active IC components such as the beamformer ICs (BFICs).

LE-DPAM combines fused deposition modeling (FDM) for extrusion of thermoplastic dielectric materials and micro-dispensing of conductive layers. Additionally, LE-DPAM platform includes micro-milling and laser micro-machining capabilities to serve as subtractive manufacturing utilized for reducing surface roughness, creating vias, refining the dimensions of the signal lines and increasing conductivities of micro-dispensed inks/pastes [7]. In a recent conference paper [8], we reported the progress in packaging mm-wave BFICs using LE-DPAM through preliminary 3D printed board-level design. In this paper, we first present the manufactured test board through use of LE-DPAM and report its experimentally characterized performance within the 24 GHz - 28 GHz band. Subsequently, we present the design and performance of a 2×2 mm-wave antenna array with a corporate feeding network that is fully printed by using LE-DPAM. The characterized performances from these separate board and antenna level demonstrations show the promise of LE-DPAM towards structural integration of mm-wave PAAs.

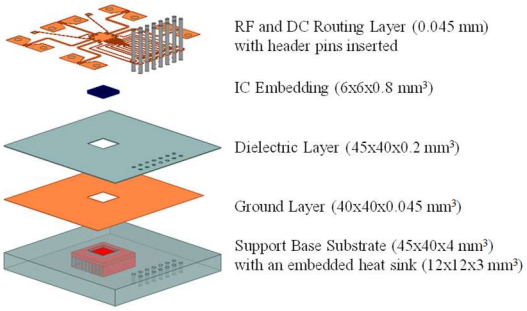

Fig. 1. Layer structure of the LE-DPAM BFIC package assembly.

II. Board Level BFIC Packaging Using LE-DPAM

For this work, Acrylonitrile Butadiene Styrene (ABS) polymer filament is adopted as the feedstock material for the substrate. The dielectric constant and loss tangent are 2.51 and 0.0045, respectively. Silver conductive ink (Dupont CB028) is employed for printing conductive layers. The conductivity for CB028 ink is 1.8×10^6 S/m. The BFIC board assembly comprises a total of four layers as depicted in Fig. 1. The support layer, with a thickness of 4 mm, is positioned at the bottom. The ground layer is micro-dispensed onto the support layer, followed by printing of the dielectric layer. After utilizing milling to smoothen the surface and achieve the desired thickness of 0.2 mm, the RF and DC circuits are micro-dispensed and refined through laser micromachining.

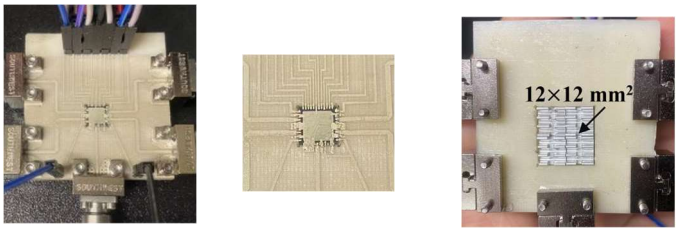

(a) (b) (c)

Fig. 2. Top-views of BFIC integration package: (a) entire assembly, (b) close-up view of interconnects, and (c) embedded heat sink on back.

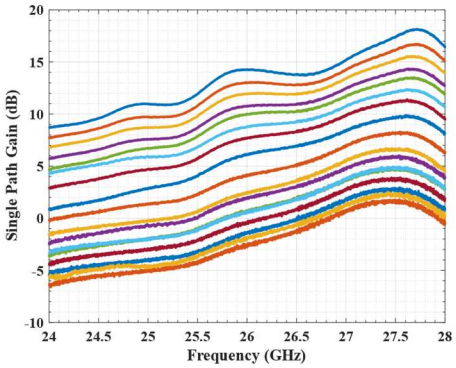

Fig. 3. Meaured single path gain control for one of the four BFIC channels.

The BFIC board manufactured using LE-DPAM is shown in Fig. 2. Fig. 3 and 4 present the measured gain and phase from the board for one of the RF ports (channels) when the BFIC is operated in its receive mode. Different ports and transmit mode operation provide similar characteristics to those seen in Fig. 2 and Fig. 3, and therefore not presented for brevity. In receive mode, the BFIC supply voltage is 1.8 V, and the measured supply current is 200 mA. The BFIC employed in design exhibits four mm-wave channels to support four single polarized antennas in both transmit (Tx) and receive (Rx) modes. Along with Tx/Rx path selection switches, each mm-wave channel also incorporates amplification, attenuation, and phase shifting capability. Due to the integrated amplification that contributes to 1.8 × 0.2 = 0.36 W of DC power consumption, thermal management becomes important for BFICs. As shown in Fig 2(c), a 12×12 mm^2 aluminum heat sink was used to prevent over-heating. Fig. 3 shows the measured gain from one of the mm-wave channels when 32 different attenuation settings are applied. At 0 dB attenuation, the maximum measured gain is 18 dB. The microstrip line loss for the shown board is characterized as 0.166 dB/mm at 26.5 GHz [8]. The total line length of 25 mm leads to a loss of 4.15 dB. The total gain of each single mm-wave channel is therefore ~22 dB. Fig. 4 depicts six different phase control states on the same mm-wave channel out of 32 different states available and it is in accordance with manufacturer specifications.

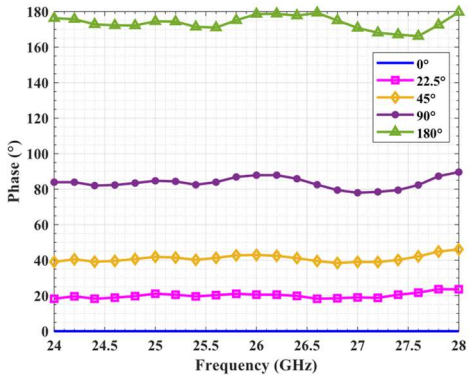

Fig. 4. Measured phase of six sample states for one of the four channels.

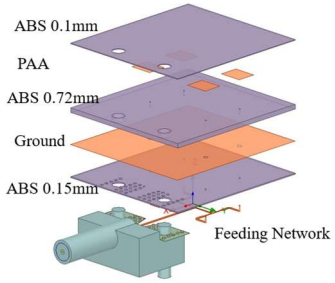

Fig. 5. Layered structure of the standalone corporate-fed 2×2 antenna array.

III. MM-WAVE ANTENNA ARRAY USING LE-DPAM

To assess the viability of employing LE-DPAM for constructing a mm-wave antenna array that will eventually be built over the BFIC in an integrated manner, we investigated the performance of a passive broad-side radiating 2×2 patch antenna array. Fig. 5 shows the substrate stack up of the antenna array that is printed starting from the top layer towards the bottom layer. ABS is employed as the substrate material. CB028 silver ink is utilized for all conductor layers. The corporate feed network is micro-dispensed last, becoming an exposed layer for a convenient mm-wave edge connector access. The 0.1 mm thick layer of ABS is utilized as the support layer to microdispense CB028 ink to form the patch antennas.

The patch antenna sizes are 3.45×3.35 mm^2. The antenna substrate is 0.72 mm thick. The corporate feed network is designed in a conventional way by employing quarter-wave transformers to maintain impedance matching. Fig. 6 depicts the details of the corporate feed network. The antennas are fed through vertical vias that originate from the feeding network layer. These vias, which have a diameter of 0.3 mm, penetrate through two layers of dielectric material and one ground layer.

This work was supported in part by the Army Research Laboratory Grant W911NF2020228 and in part by L3Harris Technologies Inc., Melbourne, FL, USA, under Grant A000587314.

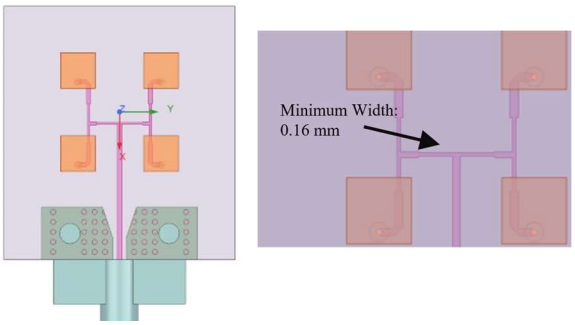

Fig. 6. Illustration of the standalone 2×2 antenna array model with corporate feed network.

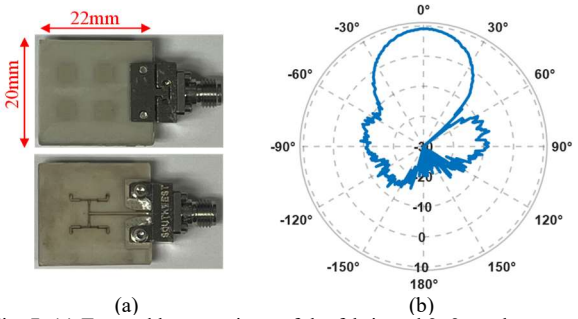

(a) (b)

Fig. 7. (a) Top and bottom views of the fabricated 2×2 patch antenna array, and (b) its measured H-plane gain pattern at 26 GHz.

Fig. 7(a) displays the fabricated standalone patch antenna array featuring the RF end launch connector. The prototype dimensions are 20×22 mm^2. Due to the slightly transparent nature of the ABS material, the patches beneath the 0.1 mm ABS support layer remain visible from one side. On the other side lies the corporate feed network, which is micro-dispensed using silver ink and precisely trimmed through the utilization of laser beams. Silver epoxy was applied on top of the connector signal pin and between the ground area of the connector and the ground plane of the prototype to improve the connection robustness. Fig. 7(b) shows the measured H-plane gain pattern. The measured broadside gain reaches 9 dB at 26 GHz and the side lobe level is below -8.5dB, whereas the simulated maximum gain at 26 GHz is 10.1 dB. The connector used in measurement has minimum of 0.5 dB loss based on manufacturer's test data. Therefore, a good agreement is achieved.

V. Conclusion

A BFIC board-level assembly and a standalone 2×2 antenna array, both operating at a center frequency of 26 GHz, are realized using LE-DPAM. The BFIC board is measured with 5-bit gain and phase controls for four antenna channels. The standalone antenna array prototype achieves a maximum gain of 9 dB with low sidelobe levels. Both components are manufactured in preparation for integrating the antenna array on top of the BFIC. Although a heat sink is embedded in the BFIC assembly, it may not be the ideal design choice. The flexibility of LE-DPAM offers numerous possibilities that we will further be investigated in our future works.

References

[1] D. Helena, A. Ramos, T. Varum and J. N. Matos, "Antenna Design Using Modern Additive Manufacturing Technology: A Review," in IEEE Access, vol. 8, pp. 177064-177083, 2020, doi: 10.1109/ACCESS.2020.3027383.

[2] M. I. M. Ghazali, S. Karuppuswami, S. Mondal, A. Kaur and P. Chahal, "Embedded Actives Using Additive Manufacturing for High-Density RF Circuits and Systems," in IEEE Transactions on Components, Packaging and Manufacturing Technology, vol. 9, no. 8, pp. 1643-1651, Aug. 2019, doi: 10.1109/TCPMT.2019.2898979.

[3] M. T. Craton, J. D. Albrecht, P. Chahal and J. Papapolymerou, "Additive Manufacturing of a Wideband Capable W-Band Packaging Strategy," in IEEE Microwave and Wireless Components Letters, vol. 31, no. 6, pp. 697-700, June 2021, doi: 10.1109/LMWC.2021.3061614.

[4] O. A. Peverini, M. Lumia, G. Addamo, G. Virone and N. J. G. Fonseca, "How 3D-Printing Is Changing RF Front-End Design for Space Applications," in IEEE Journal of Microwaves, vol. 3, no. 2, pp. 800-814, April 2023, doi: 10.1109/JMW.2023.3250343.

[5] M. Kacar, T. M. Weller and G. Mumcu, "3D Printed Wideband Multilayered Dual-Polarized Stacked Patch Antenna With Integrated MMIC Switch," in IEEE Open Journal of Antennas and Propagation, vol. 2, pp. 38-48, 2021, doi: 10.1109/OJAP.2020.3041959.

[6] M. Kacar, J. Wang, G. Mumcu, C. Perkowski, K. Church; B. Wu, and T. Weller, "Phased Array Antenna Element with Embedded Cavity and MMIC using Direct Digital Manufacturing," 2019 IEEE International Symposium on Antennas and Propagation and USNC-URSI Radio Science Meeting, Atlanta, GA, USA, 2019, pp. 81-82, doi: 10.1109/APUSNCURSINRSM.2019.8888323.

[7] M. Kacar, T. Weller and G. Mumcu, "Conductivity Improvement of Microdispensed Microstrip Lines and Grounded Coplanar Waveguides Using Laser Micromachining," in IEEE Transactions on Components, Packaging and Manufacturing Technology, vol. 10, no. 12, pp. 2129-2132, Dec. 2020, doi: 10.1109/TCPMT.2020.3038332.

[8] R. Liu, J. Braun, G. Mitchell, J. Wang and G. Mumcu, "Packaging of a Beamforming IC by Laser Enhanced Direct Print Additive Manufacturing (LE-DPAM)," 2022 3rd URSI Atlantic and Asia Pacific Radio Science Meeting (AT-AP-RASC), Gran Canaria, Spain, 2022, pp. 1-3, doi: 10.23919/AT-AP-RASC54737.2022.9814384.